International Journal of Innovative Research and Scientific Studies, 8(3) 2025, pages: 2454-2465

IJIRSS
International Journal of Innovative Research & Scientific Studies

ISSN: 2617-6548

URL: www.ijirss.com

Creation of an algorithm for the 3D modeling of manipulator motion and forward positional kinematics

Dauren Baltabay[1,2*], Muratulla Utenov[1], Tarek Sobh[3], Sichen Yuan[4], Zhadyra Zhumasheva[1]

[1]*Al-Farabi Kazakh National University, Almaty, Kazakhstan.*
[2]*L.N. Gumilyov Eurasian National University, Astana, Kazakhstan.*
[3]*Lawrence Technological University, Southfield, MI, U.S.A.*
[4]*The University of Alabama, Tuscaloosa, AL, U.S.A.*

Corresponding author: Dauren Baltabay (*Email: baltabai_dk_1@enu.kz*)

Abstract

In recent years, the utilization of 3D modeling for various robotic systems has gained significant traction, serving educational, research, and diverse applications. Presently, there are a multitude of 3D modeling tools tailored to different facets of robotic research, each possessing distinct advantages and limitations. This paper presents the development of novel algorithms and software aimed at constructing 3D representations of robotic arms that have enabled the visualization of the manipulator and its links' motion. These algorithms allow for the depiction of forward kinematic outcomes through spatial 3D graphs. Consequently, these graphical representations provide a tangible means to observe the changes in module components and parameter orientations as the manipulator assumes different spatial configurations. Within the Maple environment, a comprehensive 3D model of robotic arms was constructed, and the forward kinematic problem was solved for a manipulator that had five degrees of freedom (DoF). This endeavor was achieved by implementing the Denavit-Hartenberg method to elucidate kinematic characteristics and the Newton-Euler method to ascertain the velocity and acceleration of the robot manipulator's links. The newly created algorithms and software are expected to be widely used in 3D modeling of robotic manipulators as scientific research in industries and other complex mechanical systems.

Keywords: 3D model, Computer modeling, Kinematics, Manipulators, Maple, Positional problems.

DOI: 10.53894/ijirss.v8i3.7026
Funding: This research is funded by the Science Committee of the Ministry of Science and Higher Education of the Republic of Kazakhstan (Grant Number: AP22686476).
History: Received: 25 March 2025 / **Revised:** 29 April 2025 / **Accepted:** 1 May 2025 / **Published:** 14 May 2025

Competing Interests: The authors declare that they have no competing interests.
Authors' Contributions: All authors contributed equally to the conception and design of the study. All authors have read and agreed to the published version of the manuscript.
Transparency: The authors confirm that the manuscript is an honest, accurate, and transparent account of the study; that no vital features of the study have been omitted; and that any discrepancies from the study as planned have been explained. This study followed all ethical practices during writing.
Publisher: Innovative Research Publishing

1. Introduction

Robotic manipulators are becoming increasingly prevalent in industry, with the primary aim of enhancing human comfort, improving working conditions, and increasing productivity [1]. A robot manipulator is a mechanism that has one end connected to a base while the other end is free and equipped with a tool, enabling movement and orientation of objects within the manipulator's service areas in three-dimensional space. These manipulators, which are based on spatial mechanisms with multiple degrees of freedom (DoF), perform tasks in environments that are inaccessible or hazardous to humans and provide auxiliary functions in industrial production [2]. In a more specific context, a manipulator is often referred to as a mechanical or robotic arm [3].

Computer 3D modeling of robot manipulator motion represents a promising avenue in the investigation of spatial mechanisms. Applications of 3D modeling for robot manipulators span from prototyping and testing new designs to creating simulations for training and developing control algorithms for robotic motion. This tool is crucial for engineers and designers working in robotics, as it enables the development of more sophisticated and functional robotic systems across various industries, including manufacturing, healthcare, and education.

The innovation in 3D modeling of robotic arm movement lies in its capacity to generate accurate and realistic simulations of a robotic arm in motion. This technology allows engineers and designers to test and refine their robotic arm designs within a virtual environment before constructing a physical prototype, resulting in time and cost savings as well as improved safety and reliability of the final product. Historically, the development of robotic systems necessitated the creation of physical prototypes and their subsequent testing in laboratories or factories. This approach was not only expensive and time-consuming but also frequently resulted in design flaws and safety issues that could have been averted through more comprehensive testing.

It should be noted that this paper, along with developing an algorithm and program for building a 3D model of manipulator movement, also considers solving forward positional kinematics. An essential aspect of moving manipulator kinematics is the illustration of the obtained results in the form of 3D graphs, enabling visual observation of the results when studying kinematics, dynamics, power aspects, and manipulator control aspects, as well as planning the trajectory of the manipulator's end effector.

In most cases, 3D modeling of spatial manipulator movement and kinematics is performed in various software environments, which is considered less efficient and more time-consuming [4]. Typically, 3D models of mechanisms are created (in most cases, non-moving models) in CAD (Computer-aided design) programs and then imported into mathematical program environments for kinematic or dynamic analysis, with results obtained in the form of planar graphs.

Modern scientific literature focuses on the optimal modeling of spatial manipulators. As noted earlier, computer 3D modeling and solving forward positional kinematics of manipulators have been discussed by scientists and have received some solutions. Sánchez et al. [5] implemented Denavit-Hartenberg (D-H) methods to tackle the forward kinematics of a robotic manipulator with five DoF in a MATLAB software environment. The results of that analysis were represented in numeric values, and the manipulator's simulation was created using the ModelSim 6.3 tool, but without any movement of the manipulator. Yuan et al. [6] developed an algorithm that minimized the maximum step size of joint motions for optimal kinematics planning of a seven-DoF robot arm, with a force feedback control algorithm being added in their subsequent work. Ikeda et al. [7] modeled the kinematics and dynamics of a manipulator in constrained motion, using a planar two-DoF manipulator as an example, and compared the computational and experimental outcomes. Sherstnev et al. [8] solved the forward kinematical position problem using the D-H method and calculated the orientation and position of the tool connected to the manipulator's end effector; however, the results were not demonstrated in the form of numbers or graphs. Cui et al. [9] also utilized D-H parameters to conduct forward and inverse kinematic analysis of a 3D-modeled agricultural fruit-harvesting robot manipulator with four DoF, illustrating the results in linear charts and demonstrating the trajectory of the manipulator's end effector as planar graphs. The spatial model of this manipulator was created in the Adams environment. Haug [10] performed a kinematic analysis of a manipulator with four DoF and obtained results only in numeric form using linear algebra and calculation methods. Ge [11] proposed conducting this type of analysis using the Newton-Raphson method for a manipulator with seven DoF in a MATLAB environment, simulating the model using the MATLAB robotics toolbox, and demonstrating the solutions as linear graphs.

A forward kinematic analysis of Puma 560 (six DoF), ABB ARB 140 (six DoF), and Kuka LBR IIWA14 R820 (seven DoF) manipulators was presented by Singh and Banga [12], applying D-H parameters in a MATLAB program. In addition, they solved inverse kinematics, simulated these manipulators in the robotics toolbox, and illustrated the obtained outcomes as graphs of trajectory planning, velocity, and acceleration of the optimized trajectory of such manipulators. Chen, et al. [13] carried out forward and inverse kinematics IP of a SCARA (Selective Compliance Articulated Robot Arm) robot manipulator using D-H methods, demonstrating the solutions in numeric form, and creating an experimental system to evaluate the performance of the designed forward and inverse kinematics IP for the SCARA robot manipulator. Regassa and Zhao [14] solved the forward kinematics of a robotic manipulator with six DoF using D-H parameters, created a manipulator 3D model in the SolidWorks environment, and then transferred that model to the Virtual Universe Pro (Irai) platform to control manipulation. Winston and Jamali [15] developed a new algorithm for a two-m-link hyper-redundant axis robotic manipulator in 3D. The outcomes of inverse kinematics were numerically and graphically presented, validated by comparing the results of this study to previous research, and simulated in the Maple program. A novel method of constructing a 3D model of manipulators was represented by Tingzho et al. [16] that implemented a UR5 manipulator with six DoF. The method was carried out by the MATLAB software, modeling software from SolidWorks, Robotics Toolbox, MATLAB GUI interaction design, 3D animation, and the displayed technology of MATLAB. The animation of the manipulators was illustrated in the form of 3D graphs.

In summary, most previous scientific works describe solutions for forward and inverse kinematic analysis of various manipulators with different degrees of freedom (from three to seven) by applying several methods, with more than half of them implementing Denavit-Hartenberg parameters. However, not all of them used analytical methods to solve the kinematics. Furthermore, the modeling of the spatial manipulators under study was illustrated in a few papers, but only one of them had the ability to move within its own work area. The motion of spatial manipulators could directly display most details and results from every perspective.

As for the obtained kinematic results, half of the papers demonstrated only numeric and tabular values, which could not be visually observed for any gained solutions. For this reason, this paper focuses on developing algorithms and programs to create spatial motion 3D models as well as solving the forward positional kinematics of such 3D models of manipulators within the same program environment. Kinematics are determined by implementing Denavit-Hartenberg, Newton-Euler, and analytical methods. The 3D motion model of the manipulator is generated in the Maple math environment. The highlights of this paper are that the algorithms and programs created provide the ability to build different 3D models of manipulators that can be moved and controlled by generalized coordinates. Furthermore, the analytical method provides the most accurate outcomes compared to other methods and offers an opportunity to receive generalized characteristics during the design process. The contributions of this research to the engineering and manufacturing fields are significant, particularly in enhancing the design, analysis, and optimization of robotic systems. By integrating the development of algorithms and software that generate 3D spatial motion models of manipulators, the research provides a much-needed visual and interactive approach to solving complex kinematic problems. This allows engineers and manufacturers to better understand the behavior and motion of robotic arms within real-world environments. The ability to accurately simulate and control manipulators in 3D with generalized coordinates greatly improves the efficiency of the design process, reduces the need for costly physical prototypes, and enhances precision in tasks such as assembly, automation, and material handling. Moreover, the research offers a method for obtaining more accurate analytical outcomes, providing valuable insights into manipulator performance and enabling more informed decisions during the development of robotic systems for industrial applications [17].

Building a 3D model of manipulator movement and solving kinematics in a single Maple programming environment is a more convenient, affordable, and productive way to conduct research, and the results are presented in the form of 3D graphs. Such graphs allow for visual observation of how the modules and directions of the given manipulator parameters change in the graph, depending on the manipulator's position in space.

2. Computer 3D Modeling of Spatial Manipulators

Modeling and assembling of links and connections for manipulators were performed using operators in the Maple software environment. Maple has many possibilities for creating a moving 3D model and demonstrating the movement of each link from all sides of the manipulators in space, as well as conducting kinematic and dynamic analysis in the same program to show changes and results.

In this section, an example of this research was taken by an RRRRT manipulator with five DoF, four rotational, and one translational, which can be implemented in almost all spheres of manufacturing, engineering, and so on.

Because the axes of kinematic links are mutually perpendicular and parallel, it is possible to use the method of constructing a coordinate system proposed by J. Denavit and R. Hartenberg in the formation of coordinate manipulator link systems. To create a fully functional, visualized moving manipulator model with the given laws of generalized coordinates of a manipulator, it is necessary to combine all parts of the manipulator into one system by using programs in the Maple environment while also specifying the main connections between them.

For kinematic analysis and building a model of spatial mechanisms, it is necessary first to form the coordinate systems of the manipulator links. The formed coordinate systems of the RRRRT manipulator's links are shown in Figure 1. Secondly, it is necessary to construct the parameters of the kinematic pairs of the manipulator under study. These parameters for the RRRRT manipulator are represented in Table 1.

Table 1.
Parameters of kinematic pairs for the RRRRT manipulator.

Kinematic pairs	Links forming kinematic pairs	Types of Kinematic Pairs	The value of the parameters			
			θ_i	d_i	a_i	α_i
1	0,1	Rotational	θ_1	0.85	0	$\frac{\pi}{2}$
2	1,2	Rotational	θ_2	-0.09	0.85	0
3	2,3	Rotational	θ_3	-0.09	0	$-\frac{\pi}{2}$
4	3,4	Rotational	θ_4	0.85	0	0
5	4,5	Translational	0	d_5	0	0

According to Table 1, we can observe that the generalized coordinates of the RRRRT manipulator are the following parameters: $\theta_1, \theta_2, \theta_3, \theta_4, d_5$.

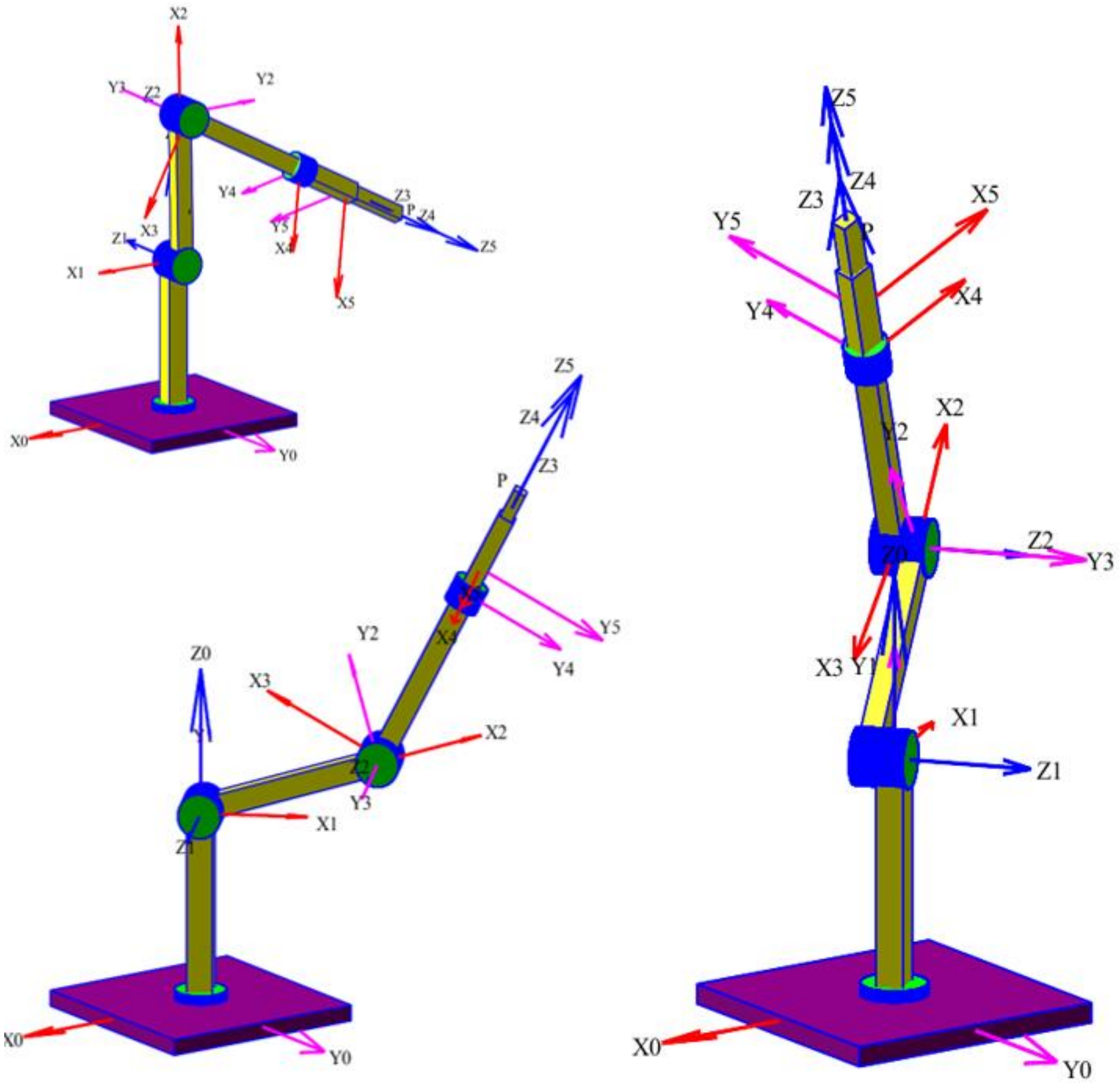

Figure 1.
3D motion model of the RRRRT manipulator in several positions.

3. A Forward Positional Kinematics Solution of Spatial Manipulators

In this section, the forward positional kinematics problem of this spatial manipulator is studied in detail. To find the kinematic characteristics of the manipulator, the Denavit-Hartenberg and Newton-Euler methods were rationally implemented. The received matrix, equations of linear and angular velocity, and acceleration were solved by the analytical method using the Maple environment.

A special choice of coordinate systems for the manipulator links allows using only four parameters (not six, as in the general case) to describe the transition from one system to another. The system $O_{i-1}X_{i-1}Y_{i-1}Z_{i-1}$ can be transformed into the system $O_iX_iY_iZ_i$ by means of rotation, two transfers, and one more rotation performed in the following order:

1) $R(Z_{i-1}, \theta_i)$ is a rotation of the system $O_{i-1}X_{i-1}Y_{i-1}Z_{i-1}$ around the axis Z_{i-1} by an angle θ_i until the axis X_{i-1} becomes parallel to the axis X_i. This motion can be described by a homogeneous matrix elementary rotation:

$$R(Z_{i-1},\theta_i)=\begin{bmatrix}\cos(\theta_i) & -\sin(\theta_i) & 0 & 0\\ \sin(\theta_i) & \cos(\theta_i) & 0 & 0\\ 0 & 0 & 1 & 0\\ 0 & 0 & 0 & 1\end{bmatrix} \quad (1)$$

2) $TZi{-}1,di$ is the transfer of the rotated system along the $Zi{-}1$ axis by the value si until the $Xi{-}1$ and Xi axes are on the same straight. Then the homogeneous matrix of the elementary shift has the form

$$T(Z_{i-1},d_i)=\begin{bmatrix}1 & 0 & 0 & 0\\ 0 & 1 & 0 & 0\\ 0 & 0 & 1 & d_i\\ 0 & 0 & 0 & 1\end{bmatrix}. \quad (2)$$

3) $TXi{-}1,ai$ is the transfer along the Xi axis by the value ai until the origin of coordinates coincide. The homogeneous matrix of the elementary shift in this case is equal to:

$$T(X_{i-1},a_i)=\begin{bmatrix}1 & 0 & 0 & a_i\\ 0 & 1 & 0 & 0\\ 0 & 0 & 1 & 0\\ 0 & 0 & 0 & 1\end{bmatrix} \quad (3)$$

4) $R(Xi,\alpha i)$ is rotation around the Xi axis by an angle αi until the $Zi{-}1$ axis is aligned with the Zi axis. This action is described by a homogeneous rotation matrix:

$$R(X_i,\alpha_i)=\begin{bmatrix}1 & 0 & 0 & 0\\ 0 & \cos(\alpha_i) & -\sin(\alpha_i) & 0\\ 0 & \sin(\alpha_i) & \cos(\alpha_i) & 0\\ 0 & 0 & 0 & 1\end{bmatrix} \quad (4)$$

The parameter d_i is the distance from the beginning of the $O_{i-1}X_{i-1}Y_{i-1}Z_{i-1}$ coordinate system to the intersection of the Z_{i-1} axis with the X_i axis, counted along the Z_{i-1} axis; if the kinematic pair $(i-1,i)$ is translational, then d_i is a generalized coordinate; a_i is the distance between the intersection of the Z_{i-1} axis with the X_i axis and the beginning of the $O_iX_iY_iZ_i$ coordinate system, measured along the X_i axis; θ_i is the angle by which the X_{i-1} axis must be rotated around the Z_{i-1} axis so that it becomes co-directed with the X_i axis. If the kinematic pair $(i-1,i)$ is rotational, then θ_i is a generalized coordinate; α_i is equal to the angle of rotation of the Z_{i-1} axis around the X_i axis until it coincides with the Z_i axis.

The resulting transition matrix connecting the systems $O_{i-1}X_{i-1}Y_{i-1}Z_{i-1}$ and $O_iX_iY_iZ_i$ is the product of the above matrices:

$A_i^{i-1}=R(Z_{i-1},\theta_i)T(Z_{i-1},s_i)T(X_{i-1},a_i)R(X_i,\alpha_i)$ or

$$A_i^{i-1}=\begin{bmatrix}\cos(\theta_i) & -\sin(\theta_i)\cos(\alpha_i) & \sin(\theta_i)\sin(\alpha_i) & a_i\cos(\theta_i)\\ \sin(\theta_i) & \cos(\theta_i)\cos(\alpha_i) & -\cos(\theta_i)\sin(\alpha_i) & a_i\sin(\theta_i)\\ 0 & \sin(\alpha_i) & \cos(\alpha_i) & s_i\\ 0 & 0 & 0 & 1\end{bmatrix}. \quad (5)$$

The matrix A_i^{i-1} is written in the following form.

$$A_i^{i-1}=\begin{bmatrix}R_i^{i-1} & \vec{O}_i^{i-1}\\ 0 & 1\end{bmatrix}, \quad (6)$$

where

$$R_i^{i-1}=\begin{bmatrix}\cos(\theta_i) & -\sin(\theta_i)\cos(\alpha_i) & \sin(\theta_i)\sin(\alpha_i)\\ \sin(\theta_i) & \cos(\theta_i)\cos(\alpha_i) & -\cos(\theta_i)\sin(\alpha_i)\\ 0 & \sin(\alpha_i) & \cos(\alpha_i)\end{bmatrix}. \quad (7)$$

R_i^{i-1} matrix determines the orientation of the axes of the $O_iX_iY_iZ_i$ coordinate system relative to the $O_{i-1}X_{i-1}Y_{i-1}Z_{i-1}$ coordinate system

$$\vec{O}_i^{i-1}=\begin{bmatrix}a_i\cos(\theta_i)\\ -a_i\sin(\theta_i)\\ s_i\end{bmatrix}, \quad (8)$$

$\vec{O}_i^{i-1}$ vector characterizes the position of the origin point of the $O_iX_iY_iZ_i$ coordinate system in the reference frame $O_{i-1}X_{i-1}Y_{i-1}Z_{i-1}$.

Using the matrix A_i^{i-1}, it is possible to link the radius vectors of the same point in the $O_{i-1}X_{i-1}Y_{i-1}Z_{i-1}$and $O_iX_iY_iZ_i$ systems:

$$\vec{r}_i^{i-1} = A_i^{i-1}\vec{r}_i^{i}, \qquad (9)$$

where $\vec{r}_i^i = [x_i \quad y_i \quad z_i \quad 1]^T$ is a column matrix defining the position of an arbitrary point of a i link in the reference frame $O_iX_iY_iZ_i$, rigidly connected to this link; $\vec{r}_i^{i-1} = [x_{i-1} \quad y_{i-1} \quad z_{i-1} \quad 1]^T$ is a column matrix defining the position of the same point in the system $O_{i-1}X_{i-1}Y_{i-1}Z_{i-1}$, rigidly connected to the $i-1$ link.

The position and orientation of the i-th link of the manipulator in the reference frame $O_0X_0Y_0Z_0$ associated with the rack is determined as follows [18]:

$$A_i^0 = A_1^0A_2^1A_3^2 \ldots A_i^{i-1} = \begin{bmatrix} R_i^0 & \vec{O}_i^0 \\ 0 & 1 \end{bmatrix}. \qquad (10)$$

where

$$R_i^0 = \begin{bmatrix} A_i^0(1,1) & A_i^0(1,2) & A_i^0(1,3) \\ A_i^0(2,1) & A_i^0(2,2) & A_i^0(2,3) \\ A_i^0(3,1) & A_i^0(3,2) & A_i^0(3,3) \end{bmatrix}, \qquad (11)$$

$$\vec{O}_i^0 = \begin{bmatrix} A_i^0(1,4) \\ A_i^0(2,4) \\ A_i^0(3,4) \end{bmatrix}. \qquad (12)$$

The left sub-matrix R_i^0 of the matrix A_i^0 represents the direction cosine, respectively, of the axes $X_iY_iZ_i$ in the reference frame $O_0X_0Y_0Z_0$. The vector $\vec{O}_i^0$ defines the position of the origin point of the coordinate system $O_iX_iY_iZ_i$ in the reference frame $O_0X_0Y_0Z_0$.

Thus, the solution to determining the position of the manipulator links boils down to the fact that the given values of generalized coordinates, the values of the elements of the matrix A_i^0 are calculated using (1) and therefore, according to (5), the position and orientation of the i-th link in the coordinate system $O_0X_0Y_0Z_0$, rigidly connected to the manipulator rack are determined.

Denote by $\vec{r}_i^i = [x_i^i \quad y_i^i \quad z_i^i \quad 1]^T$ vector of homogeneous coordinates of a point of a solid body in the associated $O_iX_iY_iZ_i$ coordinate system and the transition matrix A_i^0 to the stationary system $O_0X_0Y_0Z_0$. Then the following relation takes place:

$$\vec{r}_i^0 = A_i^0\vec{r}_i^i, \qquad (13)$$

where

$\vec{r}_i^0 = [x_i^0 \quad y_i^0 \quad z_i^0 \quad 1]^T$ is a homogeneous position vector, points $\vec{r}_i^i = [x_i^i \quad y_i^i \quad z_i^i \quad 1]^T$ of a solid body in a bound $O_iX_iY_iZ_i$ coordinate system, in a fixed $O_0X_0Y_0Z_0$ coordinate system.

The angular velocity $\vec{\omega}_i$ of the i-th link relative to the base coordinate system is represented as follows [18]:

$$\vec{\omega}_i = \begin{cases} \vec{\omega}_{i-1} + R_{i-1}^0\vec{z}_0\dot{q}_i, \text{if the } i-\text{th kinematic pair is rotational,} \\ \vec{\omega}_{i-1}, \text{if the } i-\text{th kinematic pair is translational,} \end{cases} \qquad (14)$$

where i=1,2,…,n, $\vec{z}_0 = (0,0,1)^T$.

Then the angular acceleration $\vec{\varepsilon}_i$ of the i-th link relative to the base coordinate system is determined by the expression:

$$\vec{\varepsilon}_i = \begin{cases} \vec{\varepsilon}_i = \vec{\varepsilon}_{i-1} + R_{i-1}^0\vec{z}_0\ddot{q}_i + \vec{\omega}_{i-1} \times (R_{i-1}^0\vec{z}_0\dot{q}_i), \\ \text{if the } i-\text{th kinematic pair is rotational,} \\ \vec{\varepsilon}_{i-1}, \text{if the } i-\text{th kinematic pair is translational.} \end{cases} \qquad (15)$$

For linear velocities and accelerations of the i-th link of the manipulator relative to the base coordinate system we have the following relations:

$$\vec{v}_i = \begin{cases} \vec{v}_{i-1} + \vec{\omega}_i \times \vec{p}_i^{i-1}, \text{if the } i - \text{th kinematic pair is rotational,} \\ \vec{v}_{i-1} + \vec{\omega}_i \times \vec{p}_i^{i-1} + R_{i-1}^0 \vec{z}_0 \dot{q}_i, \\ \text{if the i} - \text{th kinematic pair is translational.} \end{cases} \quad (16)$$

$$\vec{a}_i = \begin{cases} \vec{a}_{i-1} + \vec{\omega}_i \times \left(\vec{\omega}_i \times \vec{p}_i^{i-1}\right) + \vec{\varepsilon}_i \times \vec{p}_i^{i-1}, \\ \text{if the } i - \text{th kinematic pair is rotational,} \\ \vec{a}_{i-1} + \vec{\omega}_i \times \left(\vec{\omega}_i \times \vec{p}_i^{i-1}\right) + 2\vec{\omega}_i \times (R_{i-1}^0 \vec{z}_0 \dot{q}_i) + \vec{\varepsilon}_i \times \vec{p}_i^{i-1} + R_{i-1}^0 \vec{z}_0 \ddot{q}_i, \\ \text{if the i} - \text{th kinematic pair is translational.} \end{cases} \quad (17)$$

$\vec{p}_i^{i-1}$ - the position of the beginning of the *i*-th coordinate system relative to the beginning of the $i - 1$ coordinate system is determined by the following expression:

$$\vec{p}_i^{i-1} = \vec{p}_i^0 - \vec{p}_{i-1}^0, \quad (18)$$

where

$$\vec{p}_i^0 = \begin{bmatrix} A_i^0(1,4) \\ A_i^0(2,4) \\ A_i^0(3,4) \end{bmatrix}, \vec{p}_{i-1}^0 = \begin{bmatrix} A_{i-1}^0(1,4) \\ A_{i-1}^0(2,4) \\ A_{i-1}^0(3,4) \end{bmatrix}.$$

Linear velocities and acceleration of the point $\vec{P}_i^i = [x_i \quad y_i \quad z_i]^T$ of the *i*-th link, respectively, relative to the base coordinate system are determined by the expressions:

$$\vec{v}_{iP} = \vec{\omega}_i \times \vec{P}_i + \vec{v}_i, \quad (19)$$

$$\vec{a}_{iP} = \vec{a}_i + \vec{\omega}_i \times \left(\vec{\omega}_i \times \vec{P}_i\right) + \vec{\varepsilon}_i \times \vec{P}_i. \quad (20)$$

Analytical methods of solving the kinematics of manipulators are different from other mostly implemented methods in that they supply exact outcomes and clearly demonstrate mathematical models of the phenomenon. As for using the Maple math environment for 3D modeling, solving forward kinematic problems of manipulators and illustrating the obtained results in the form of 3D graphs could be a convenient way to do so, since almost all of the mentioned actions are performed in the same program.

4. Results and Discussion

Figures 2-8 demonstrate the results received in Maple 2023 of kinematic analysis in the form of 3D graphs of the RRRRT manipulator with kinematic characteristics for 36 positions relative to a fixed coordinate system $O_0X_0Y_0Z_0$, with the following specified values of generalized coordinates: $\theta_1 = 2\pi\sin\left(\frac{\pi}{2k} * i\right)$, $\theta_2 = -\frac{\pi}{6} + \frac{2\pi}{3}\sin\left(\frac{\pi}{2k} * i\right)$, $\theta_3 = -\frac{\pi}{2} + \frac{2\pi}{3}\sin\left(\frac{\pi}{2k} * i\right)$, $\theta_4 = \frac{2\pi}{k} * i$, $d_5 = 0.35 * \sin\left(\frac{\pi}{2k} * i\right)$, where k=36, i=0..36.

The point P of the RRRRT manipulator is connected to the coordinate system $O_5X_5Y_5Z_5$ and relatively in this system has coordinates $P_5 = [0\ 0\ 0.35]^T$. The red line in the figures is the trajectory of a point or the hodographs of angular and linear accelerations relative to the base coordinate system $O_0X_0Y_0Z_0$. Yellow and green straight lines with an arrow are vectors connecting the points of the trajectory or hodograph with the beginning of the base coordinate system.

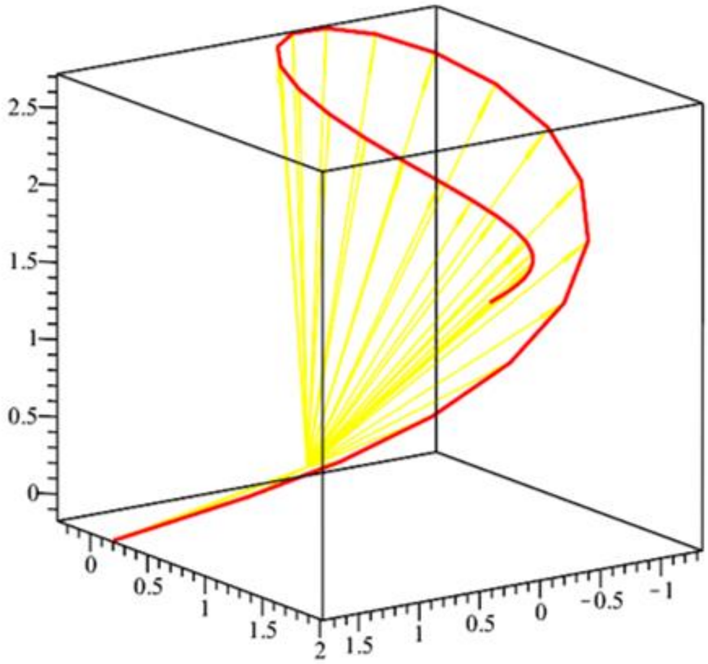

Figure 2.
Trajectory of point P for 36 positions of the manipulator RRRRT relative to the base coordinate system $O_0X_0Y_0Z_0$.

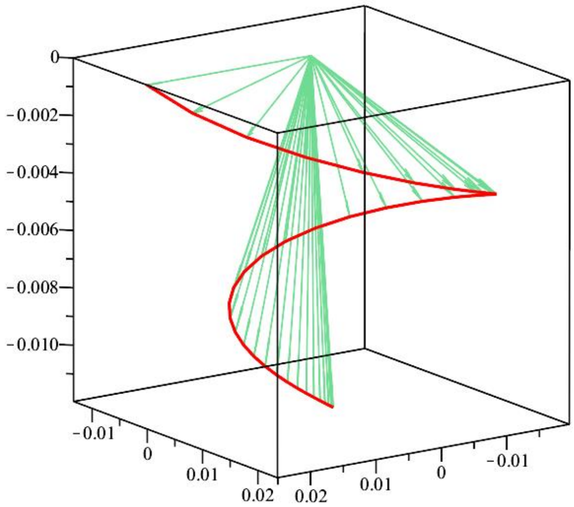

Figure 3.
Angular acceleration ε_2 of link 2 for 36 positions of the manipulator RRRRT.

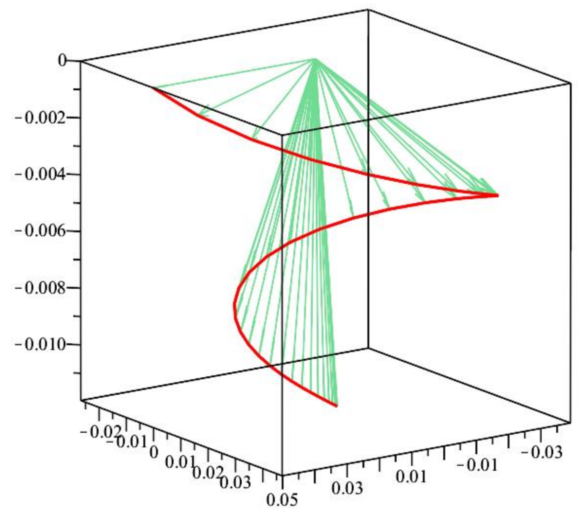

Figure 4.
Angular acceleration ε_3 of link 3 for 36 positions of the manipulator RRRRT.

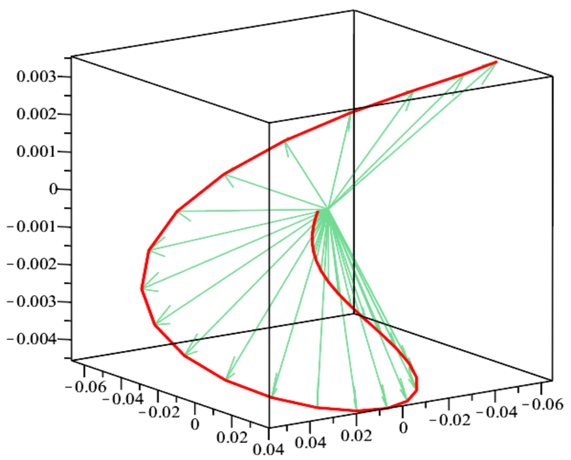

Figure 5.
Linear acceleration a_{O2} of the origin O_2 of the moving coordinate system $O_2X_2Y_2Z_2$ for 36 positions of the RRRRT manipulator.

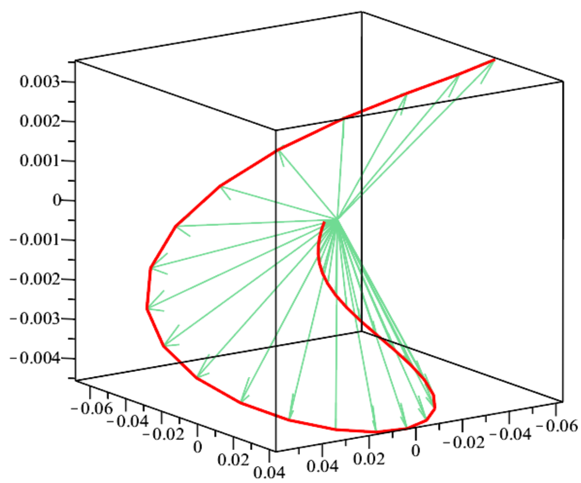

Figure 6.
Linear acceleration a_{O3} of the origin O_3 of the moving coordinate system $O_3X_3Y_3Z_3$ for 36 positions of the RRT manipulator.

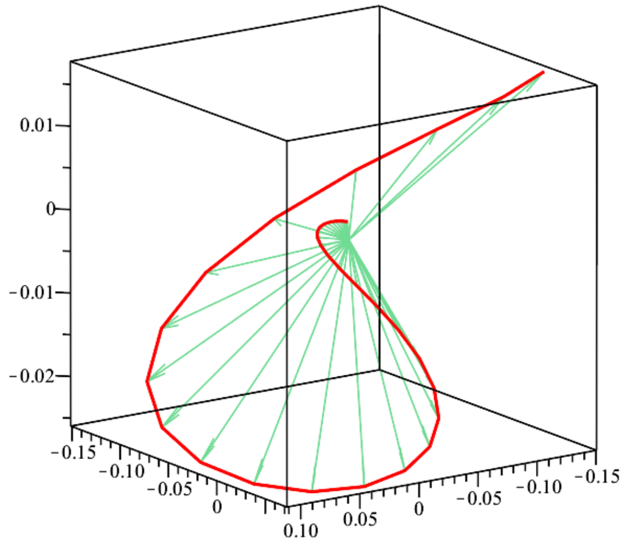

Figure 7.
Linear acceleration a_{O4} of the origin O_4 of the moving coordinate system $O_4X_4Y_4Z_4$ for 36 positions of the RRT manipulator.

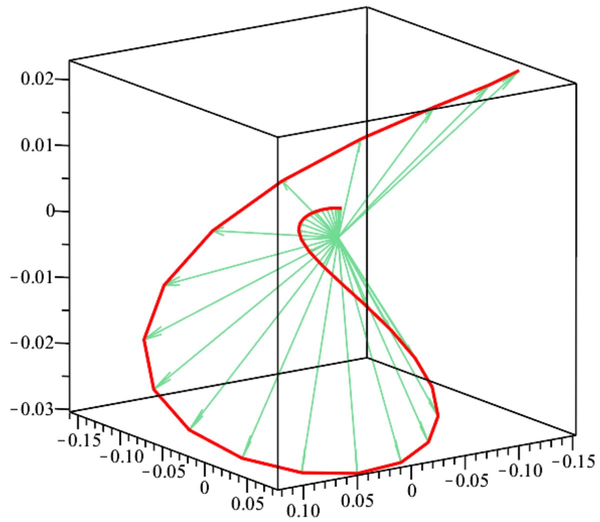

Figure 8.
Linear acceleration a_{O5} of the origin O_5 of the moving coordinate system $O_5X_5Y_5Z_5$ for 36 positions of the RRRRT manipulator.

Figure 2 illustrates the spatial trajectory of point P, fixed in the end-effector of the RRRRT manipulator, as it moves through 36 different positions with respect to the base coordinate system. The red line represents the path traced by point P, showcasing the manipulator's ability to follow a complex 3D motion. This visualization is crucial for understanding the overall movement capabilities of the manipulator, verifying the accuracy of the developed kinematic model, and optimizing its path planning.

Figure 3 - Figure 4 present the angular acceleration of link 2 and link 3 over 36 positions. The graphical representation highlights how the rotational dynamics of this link change throughout the manipulator's motion. This data is vital for analyzing the dynamic behavior of the manipulator, ensuring smooth and controlled rotational movements, and reducing potential wear on the joints due to abrupt accelerations. It also assists in refining the design to handle varying dynamic loads effectively.

Figures 5 – 7 display the linear acceleration of the origin of the moving coordinate system for all 36 positions. By showing the changes in linear acceleration, the figure helps assess the impact of different manipulator configurations on translational movements, which is essential for applications requiring precise positioning and smooth operation.

Finally, Fig. 8 shows the linear acceleration at the origin of the coordinate system X5Y5Z5, attached to the end effector. The data provides critical insights into the end effector's behavior under different operational scenarios, aiding in the fine-tuning of control parameters to achieve high precision in industrial applications such as assembly and material handling.

These figures collectively demonstrate the effectiveness of the developed algorithms and software in accurately modeling and analyzing the motion of the RRRRT manipulator. By providing a comprehensive visualization of both angular and linear accelerations, the study contributes valuable insights into optimizing manipulator design and control, which are crucial for enhancing the efficiency and reliability of robotic systems in various industrial applications.

To verify our developed algorithms and programs, we applied them to solving problems, using the created 3D moving model of the RRRRT manipulator as an example. The forward positional kinematics problem was solved, and diagrams of changes in angular and linear accelerations were constructed. Thus, we wanted to show that the algorithms and programs we developed work and to determine that angular and linear accelerations do not depend on the positional changes of mechanisms.

In this study, the vectors of linear accelerations of points and the vectors of angular accelerations of the links of this spatial manipulator were determined relative to the base and associated Denavit-Hartenberg coordinate systems using the Newton-Euler recurrent equations. The components of these vectors were ascertained for subsequent investigations. This step is crucial, as it forms the basis for comprehending various dynamic loads and discerning the underlying distribution patterns.

5. Conclusion

In many instances, as pointed out above, the 3D modeling of spatial manipulator motion and direct kinematics is conducted across different software platforms, a process that is often less efficient and more time-intensive. Commonly, non-moving 3D models of mechanisms are first developed in CAD (Computer-Aided Design) software, then imported into mathematical environments for subsequent kinematic or dynamic analysis, where the results are typically presented as two-dimensional graphs. For this reason, this study introduced novel algorithms and programs designed to construct motional 3D models of spatial manipulators. The developed system was effectively applied to models and addressed the forward kinematics of a five-DoF manipulator, showcasing the results through intricate 3D graphs. These visualizations provided clear insights into the trajectory, velocities, and accelerations of each manipulator link. The kinematics calculations were comprehensively executed employing the analytical method, Denavit-Hartenberg parameters, and Newton-Euler methods.

While the presented work emphasizes an innovative approach to generating 3D models of spatial manipulators governed by generalized coordinates, it also delineates potential directions for subsequent research. Notably, it paves the way for examining the dynamic loads, rigidity, and strength of these spatial manipulators. It is planned to continue researching the dynamic loads of this robot manipulator and implement the obtained findings.

Furthermore, the significance of the research is accentuated by the implementation of these algorithms and programs within only the Maple environment. Here, a comprehensive study encompassing kinematics, dynamics, and force analysis can be undertaken, with the resulting insights directly visualized on the manipulators. It is anticipated that this work will serve as a catalyst for further investigations and adaptations of the presented algorithms and programs to a broader range of analytical domains.

References

[1] F. L. Lewis, D. M. Dawson, and C. T. Abdallah, *Robot manipulator control: Theory and practice*. New York, USA: CRC Press, 2003.

[2] R. P. Paul, *Robot manipulators: mathematics, programming, and control: The computer control of robot manipulators*. Cambridge, MA, USA: Richard Paul, 1981.

[3] B. Saeed, *Introduction to robotics*. Upper Saddle River, NJ: Prentice Hall, 2001.

[4] H.-J. Kang and Y.-S. Ro, "Robot manipulator modeling in Matlab-SimMechanics with PD control and online gravity compensation," in *Proceedings of the International Forum on Strategic Technology*, 2010: IEEE, pp. 446-449.

[5] D. F. Sánchez, D. M. Muñoz, C. H. Llanos, and J. M. Motta, "FPGA implementation for direct kinematics of a spherical robot manipulator," in *2009 International Conference on Reconfigurable Computing and FPGAs*, 2009: IEEE, pp. 416-421.

[6] S. Yuan, H. Zhang, N. Wang, and N. Luan, "Motion study of a redundant 7-DOF operation robot," in *2011 International Conference on Electrical and Control Engineering*, 2011: IEEE, pp. 3056-3060.

[7] T. Ikeda, M. Minami, and Y. Mae, "Direct force and position control using kinematics and dynamics of manipulators in constrained motion," in *2005 IEEE/RSJ International Conference on Intelligent Robots and Systems*, 2005: IEEE, pp. 3815-3820.

[8] V. V. Sherstnev, O. E. Bezborodova, A. N. Spirkin, O. N. Bodin, and A. O. Kholudeneva, "Solving the direct kinematics problem of the mechanical manipulator of an unmanned aircraft," in *2022 IEEE 23rd International Conference of Young Professionals in Electron Devices and Materials (EDM)*, 2022: IEEE, pp. 560-563.

[9] Y. Cui, J. Hua, and P. Shi, "Kinematics simulation of an aided fruit-harvesting manipulator based on ADAMS," in *2010 International Conference On Computer Design and Applications*, 2010, vol. 5: IEEE, pp. V5-222-V5-226.

[10] E. J. Haug, "Manipulator kinematics and dynamics on differentiable manifolds: Part i kinematics," *Journal of Computational and Nonlinear Dynamics*, vol. 17, no. 2, p. 021002, 2022. https://doi.org/10.1115/1.4052652

[11] D. Ge, "Kinematics modeling of redundant manipulator based on screw theory and Newton-Raphson method," presented at the Journal of Physics: Conference Series, 2022.

[12] G. Singh and V. K. Banga, "Kinematics and trajectory planning analysis based on hybrid optimization algorithms for an industrial robotic manipulators," *Soft Computing,* vol. 26, no. 21, pp. 11339-11372, 2022. https://doi.org/10.1007/s00500-022-07423-y

[13] W.-C. Chen, C.-S. Chen, F.-C. Lee, and Y.-S. Kung, "Digital hardware implementation of the forward/inverse kinematics for a SCARA robot manipulator," in *2018 IEEE International Conference on Applied System Invention (ICASI),* 2018: IEEE, pp. 54-57.

[14] H. B. Regassa and W. Zhao, "Design and realization of 3D simulation system of 6 DOF robot manipulator based on virtual universe Pro (Irai) platform," *International Journal of Engineering Research & Technology,* vol. 9,, pp. 76–80, 2020.

[15] S. I. Winston and A. Jamali, "Axis manipulation to solve Inverse Kinematics of Hyper-Redundant Robot in 3D Space," *Journal of Integrated and Advanced Engineerin,* vol. 2, no. 2, pp. 113-122, 2022. https://doi.org/10.51662/jiae.v2i2.81

[16] N. Tingzho, F. Ling, and Z. Jingzhi, "A novel method of constructing open 3D virtual simulation platform for robots," *International Journal of Mechatronics and Applied Mechanics,* vol. 7, pp. 42–47, 2020. https://doi.org/10.17683/ijomam/issue7.6

[17] M. Utenov, D. Baltabay, and Z. Zhumasheva, "3D modeling manipulator movement and direct positional kinematic analysis," presented at the IFToMM Asian Conference on Mechanism and Machine Science, 2024.
[18] K. S. Fu, R. C. Gonzalez, and C. S. G. Lee, *Robotics: Control, sensing, vision, and intelligence*. New York, USA: McGraw-Hill, 1987.